

## Cytotoxicity of CeO<sub>2</sub> nanoparticles using in vitro assay with *Mytilus galloprovincialis* hemocytes: Relevance of zeta potential, shape and biocorona formation



M. Sendra<sup>a,\*</sup>, M. Volland<sup>a</sup>, T. Balbi<sup>b</sup>, R. Fabbri<sup>b</sup>, M.P. Yeste<sup>c</sup>, J.M. Gatica<sup>c</sup>, L. Canesi<sup>b</sup>, J. Blasco<sup>a</sup>

<sup>a</sup> Department of Ecology and Coastal Management, Institute of Marine Sciences of Andalusia (CSIC), Campus Río S. Pedro, 11510, Puerto Real, Cádiz, Spain

<sup>b</sup> Department of Earth, Environment and Life Sciences, University of Genova, Corso Europa 26, 16132, Genova, Italy

<sup>c</sup> Department of Material Science, Metallurgical Engineering and Inorganic Chemistry, Faculty of Sciences, University of Cadiz, E-11510, Puerto Real, Cádiz, Spain

### ARTICLE INFO

#### Keywords:

Immune regulation  
Mussel  
CeO<sub>2</sub> NPs  
Agglomeration  
Zeta potential  
Biocorona

### ABSTRACT

Over the last decades, the growth in nanotechnology has provoked an increase in the number of its applications and consumer products that incorporate nanomaterials in their formulation. Metal nanoparticles are released to the marine environment and they can interact with cells by colloids forces establish a nano-bio interface. This interface can be compatible or generate bioadverse effects to cells. The daily use of CeO<sub>2</sub> nanoparticles (CeO<sub>2</sub> NPs) in industrial catalysis, sunscreen, fuel cells, fuel additives and biomedicine and their potential release into aquatic environments has turned them into a new emerging pollutant of concern. It is necessary to assess of effects of CeO<sub>2</sub> NPs in aquatic organisms and understand the potential mechanisms of action of CeO<sub>2</sub> NP toxicity to improve our knowledge about the intrinsic and extrinsic characteristic of CeO<sub>2</sub> NPs and the interaction of CeO<sub>2</sub> NPs with biomolecules in different environment and biological fluids. The conserved innate immune system of bivalves represents a useful tool for studying immunoregulatory responses when cells are exposed to NPs. In this context, the effects of two different CeO<sub>2</sub> NPs with different physico-chemical characteristics (size, shape, zeta potential and Ce<sup>+3</sup>/Ce<sup>+4</sup> ratio) and different behavior with biomolecules in plasma fluid were studied in a series of in vitro assays using primary hemocytes from *Mytilus galloprovincialis*. Different cellular responses such as lysosome membrane stability, phagocytosis capacity and extracellular reactive oxygen species (ROS) production were evaluated. Our results indicate that the agglomeration state of CeO<sub>2</sub> NPs in the exposure media did not appear to have a substantial role in particle effects, while differences in shape, zeta potential and biocorona formation in NPs appear to be important in provoking negative impacts on hemocytes.

The negative charge and the rounded shape of CeO<sub>2</sub> NPs, which formed Cu, Zn-SOD biocorona in hemolymph serum (HS), triggered higher changes in the biomarker of stress (LMS) and immunological parameters (ROS and phagocytosis capacity). On the other hand, the almost neutral surface charge and well-faceted shape of CeO<sub>2</sub> NPs did not show either biocorona formation in HS under tested conditions or significant responses. According to the results, the most relevant conclusion of this work is that not only the physicochemical characterization of CeO<sub>2</sub> NPs plays an important role in NPs toxicity but also the study of the interaction of NPs with biological fluids is essential to know its behavior and toxicity at cellular level.

### 1. Introduction

In the era of nanotechnology, engineers nanoparticles (ENPs) is becoming a potential source of emerging pollutants in natural aquatic systems, with negative effects on aquatic organisms (Baker et al., 2014; Moore, 2006). CeO<sub>2</sub> NPs are known for their catalytic and redox properties (Celardo et al., 2011), these NPs are widely used in many applications such as: coatings, glass polishing agents, oxygen gas sensors, fuel cells, fuel additives, and pharmacological uses (Celardo et al.,

2011; Izu et al., 2004; Murray et al., 1999; Nguyen Quang et al., 2011; Selvan et al., 2009). Environmental concentrations of CeO<sub>2</sub> NPs have so far only been predicted by models, due to limitations in analytical methods. According to Gottschalk et al. (2015), the principal source of CeO<sub>2</sub> NPs was fly ash and the predicted concentration in surface water is in the range between 0.6–100 ng·L<sup>-1</sup>; however, the highest concentrations are found in sludge treated soils in a range of concentration between 94 and 5100 ng·kg<sup>-1</sup> (Gottschalk et al., 2015).

Due to the physicochemical properties of CeO<sub>2</sub> NPs such as their

\* Corresponding author.

E-mail address: [marta.sendra@icman.csic.es](mailto:marta.sendra@icman.csic.es) (M. Sendra).

small size, high specific surface area and low dissolution rate, they have the potential to be easily dispersed and can establish nano-bio interfaces with proteins, lipids, sugars, membranes, cells, DNA and organelles (Teske and Detweiler, 2015). The formation of this interface depends on colloidal forces and dynamic bio-physicochemical interactions which can lead to the formation of biocorona NPs, particle wrapping and intracellular uptake which may be compatible with, or generate, bioadverse processes in cells (Lynch and Dawson, 2008; Nel et al., 2009). The surface bio-transformation of metallic NPs in different natural environments and biological fluids leads to the formation of *ex vivo* and *in vivo* biocorona respectively. The biocorona can modulate the kinetic uptake of NPs into cells and cytotoxic effects in an unpredictable manner (Hadjidemetriou and Kostarelos, 2017). Furthermore, the biocorona may induce alterations in the nature of the extracellular matrix (Neagu et al., 2017). Remarkably, the constituents of the extracellular matrix interact with cell surface receptors leading to numerous signaling cascades which are closely related to healthy cell behavior (Afratis et al., 2012; Bouris et al., 2015; Gialeli et al., 2011).

In aquatic organisms, the incorporation paths of NPs can be i) direct; through the pores of the cell wall of bacteria and algae, through gills and ingestion of NP aggregates/agglomerates with organic components through the digestive system; and ii) indirect; through the physical damage of NPs in the cell wall and cell membrane. At the cellular level, NPs can be internalized by: passive diffusion, through ion channels, carrier-mediated transport, phagocytosis, micropinocytosis and through caveolar/endocytic routes. Once inside the cell, NPs can be incorporated within the functional machinery of the cells (Moore, 2006) and cause unwanted effects in aquatic organisms (Baker et al., 2014), such as: bacteria, algae (Rodea-Palomares et al., 2011; Sendra et al., 2017b), rotifers (Clément et al., 2013), crustaceans (Thit et al., 2017), gasteropod mollusks (Oliveira-Filho et al., 2016; Zhu et al., 2011), annelida (Buffet et al., 2011) and bivalves (Canesi et al., 2016a; Canesi et al., 2015; Sendra et al., 2017a); some of the effects including a reduction in swimming performance (Asghari et al., 2012), reduction in growth, reproduction (Zhao and Wang, 2011) and feeding (Croteau et al., 2011a; Croteau et al., 2011b) and dysregulation of antioxidant enzymes (García-Negrete et al., 2013; Gomes et al., 2011).

Bivalves are considered the main target group to study the effects of NPs (Canesi et al., 2012) and *in vitro* assays with mussel hemocytes represent a powerful tool to assess the immunomodulatory effect of NPs. There are some advantages: bivalves have an open circulation, with blood (hemolymph), containing circulating hemocytes, in direct contact with tissues can be easily obtained by non-invasive methods and immunotoxicity tests allow a rapid and sensitive evaluation of the effects of NPs on hemocytes (Canesi et al., 2015; Canesi et al., 2014; Canesi and Procházová, 2013; Katsumiti et al., 2016; Katsumiti et al., 2015; Shi et al., 2017; Wang et al., 2014). The innate immune system of bivalves comprises cellular and humoral components that are remarkably efficient against the entry of NPs (Canesi et al., 2016a; Canesi et al., 2012). The cellular immune system is composed by granulocytes and hyalinocytes which participate in various functions such as phagocytosis, oxyradical production, nodule formation, encapsulation, pearl formation, cytotoxicity and the synthesis and the release of microbicidal agents (Canesi et al., 2016a). The humoral components of bivalve immunity comprise soluble lectins, hydrolytic enzymes and antimicrobial peptides (Canesi et al., 2002a; Pruzzo et al., 2005). Some of the effects of nanomaterials on bivalve hemocytes are: decreased lysosomal membrane stability, lysozyme release, stimulation of an oxidative burst and NO production, induction of pre-apoptotic processes, frustrated phagocytosis, activation of P38 MAPK signaling, lipid peroxidation and DNA damage (Canesi et al., 2016a; Canesi et al., 2003; Canesi et al., 2016b; Canesi et al., 2007; Gagné et al., 2008; Gomes et al., 2013).

In a previous work performed by this research group, some CeO<sub>2</sub> NPs were characterized, two of them (identified as CNP1 and CNP2) showed intrinsic and extrinsic characteristics useful to assess the

functional parameters of immune cells. CNP1 and CNP2 were well studied and reported: i) the primary physico-chemical characteristics of CeO<sub>2</sub> NPs such as primary size, specific surface area, Ce<sup>+3</sup>/Ce<sup>+4</sup> ratio and shape (Sendra et al., 2017c), ii) behavior of CeO<sub>2</sub> NPs in different culture media to evaluate agglomeration size over time, zeta potential and scavenging of H<sub>2</sub>O<sub>2</sub> (Canesi et al., 2017; Sendra et al., 2017c) and iii) interaction of NPs with biomolecules of hemolymph leading to the formation of protein biocorona (Canesi et al., 2017).

In order to improve knowledge about the mechanisms that underlies the effects of CeO<sub>2</sub> NPs with different physicochemical properties on marine invertebrates. The novelty of this work is to assess the effects of two distinct CeO<sub>2</sub> NPs, with different intrinsic and extrinsic properties (from zeta potential, shape and biocorona formation), on primary hemocytes of *Mytilus galloprovincialis*. The hypothesis of this work was that size, surface charge, shape have a relation with interaction with biological fluids and therefore with biocorona formation of CeO<sub>2</sub> NPs. From these new acquired CeO<sub>2</sub> NPs characteristics have a direct relation with the biomarkers of stress and immunomodulatory effects of CeO<sub>2</sub> NPs in *Mytilus galloprovincialis* immune cells.

## 2. Materials and methods

### 2.1. Reagents

CeO<sub>2</sub> NPs (CAS# 643009, with 10% H<sub>2</sub>O by wt.) were obtained from Sigma Aldrich (hereafter CNP1) and CeO<sub>2</sub> NPs (CAS# US7110, with 20% H<sub>2</sub>O by wt.) were obtained from US Research Nanomaterials, Inc. (hereafter CNP2).

### 2.2. Suspensions of NPs

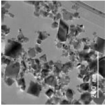
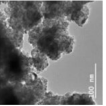
Stock suspensions of CNP1 and CNP2 were prepared in ultrapure water immediately prior to the experiments. Suspensions were tip sonicated (UP 200S Dr. Hielscher GmbH, Teltow, Germany) in an ice bath for 10 min at 100 W, and frequency of 50%. Following sonication, particle suspensions were diluted to appropriate concentrations in either ultrapure water, artificial marine water (AMW) (ASTM, 1975) or filtered (0.22 μm) hemolymph serum (HS). Control hemocytes received equal volumes of AMW or HS.

### 2.3. Primary characterization, behavior and interaction with biomolecules of CNP1 and CNP2

Details on particle size, shape, S<sub>BET</sub> and ratio Ce<sup>+3</sup>/Ce<sup>+4</sup> ratio and H<sub>2</sub>O<sub>2</sub> scavenging activity are reported in Sendra et al. (2017a,b,c) and (Canesi et al., 2017), and the results are summarized in the results section and supplementary information. Size and zeta potential were studied in ultrapure water, AMW and HS, using Dynamic Light Scattering (Zetasizer Nano ZS90, Malvern Instruments, equipped with software version 7.10) at 1 mg L<sup>-1</sup>. The agglomeration state of CeO<sub>2</sub> NPs was evaluated over time (0, 3, 6, 9, 10, 60 and 180 min) in ultrapure water and over 12 min AMW (ASTM, 1975) and HS. Zeta potential was measured in ultrapure water, AMW and HS by DLS at time zero. Polydispersity Index (PDI) was analyzed and was lower than 0.7 in all samples.

Respect to characterization of protein corona, this was performed in a previous work (Canesi et al., 2017). Briefly samples were added with SDS-sample buffer and boiled for 5 min. Proteins (10 μg) were separated by 10% SDS/PAGE for direct visualization and comparison of stained protein patterns. Bands of interests in the corona sample were cut from the gel and destained, reduced, alkylated and trypsin digested. Trypsinized peptides were analyzed by nano-HPLC-MS/MS. In parallel, samples of the pellet obtained by the centrifugation procedure containing PS-NH<sub>2</sub>-protein corona complexes, were observed by field emission scanning electron microscopy (FESEM); (Canesi et al., 2017)

**Table 1**  
Physico-chemical characteristic and behavior of CNP1 and CNP2 in ultrapure water, hemolymph filtered by 0.22  $\mu\text{m}$  and artificial marine water (pH:8.2 and IS: 720 mM). From Sendra et al. (2017a,b,c) (Canesi et al., 2017; Sendra et al., 2017c) ( $\zeta$  means zeta potential and n.d., not detected).

Primary physico-chemical properties		Behavior of CeO <sub>2</sub> NPs in different culture media													
		Ultrapure water			Hemolymph			Artificial marine water							
TEM images	Particle size by TEM (nm) <sup>y</sup>	S <sub>BET</sub> (m <sup>2</sup> /g) <sup>y</sup>	Total pore volume (cm <sup>3</sup> /g) <sup>y</sup>	Z-Avg. (nm) DLS	PdI	$\zeta$ (mV)	Z-Avg. (nm) DLS	PdI	$\zeta$ (mV)	biocorona	Z-Avg. (nm) DLS	PdI	$\zeta$ (mV)	(Ce + 3/Ce + 4) <sup>z</sup>	% Scavenging of H <sub>2</sub> O <sub>2</sub> <sup>e</sup>
	26 ± 16	42.9	0.145	106 ± 40	0.15	23.6 ± 8.3	160 ± 30	0.13	-2.6 ± 0.1	n.d.	927 ± 492	0.5	3.2 ± 0.3	0.76	76.5 ± 8.1
	9 ± 4	17.7	0.214	196 ± 64	0.08	-84 ± 4.3	250 ± 50	0.12	-10 ± 0.1	Cu, Zn-SOD	558 ± 150	0.19	-10 ± 1.8	0.92	94.3 ± 3.8

<sup>a</sup> Average data from particle size distributions obtained by TEM.

<sup>b</sup> Calculated by the BET method from the recorded nitrogen physisorption isotherms.

<sup>c</sup> Determined by the BJH method using the desorption branch of the recorded nitrogen physisorption isotherms.

<sup>d</sup> absorbance ratio Ce + 3/Ce + 4 of CeO<sub>2</sub> NPs.

<sup>e</sup> Scavenging of H<sub>2</sub>O<sub>2</sub> with respect to the total concentration 8  $\mu\text{M}$ .

#### 2.4. Animals, hemolymph collection and hemocyte treatments

Mussels (*Mytilus galloprovincialis* Lam.) 3.5–4 cm long, were purchased from an aquaculture farm (Arborea-OR, Italy) and kept for 1–3 days in static tanks containing artificial sea water (ASW) (1 L oxygenated ASW per mussel) at 16 °C. Sea water was changed daily. The hemolymph was extracted from the posterior adductor muscle of 8–20 mussels using a sterile 1 mL syringe with a 18 G1/2" needle. With the needle removed, the hemolymph was filtered through a sterile gauze and pooled in 50 mL Falcon tubes at 4 °C. Hemocyte monolayers were prepared as previously described (Canesi et al., 2008). The hemocytes were incubated at 16 °C with different concentrations of CNP1 and CNP2, depending on the endpoint measured. Short-term exposure conditions (from 30 min to 4 h) were chosen to evaluate the acute in vitro responses to CeO<sub>2</sub> NPs in analogy with previous studies with other types of NPs in mussel hemocytes (Canesi et al., 2008; Canesi et al., 2010b; Ciacci et al., 2012). Untreated (control in ASW) hemocyte samples were run in parallel (Canesi et al., 2015).

#### 2.5. In vitro assays

Hemocyte functional parameters, such as lysosomal membrane stability (LMS), phagocytosis and extracellular oxyradical production, were studied as previously described by other authors (Canesi et al., 2008; Canesi et al., 2010a; Ciacci et al., 2012). LMSL in controls and hemocytes, pre-incubated with different concentrations of CNP1 and CNP2 (1, 10 and 50 mg L<sup>-1</sup>) for 30 min, was evaluated by the Neutral Red Retention time assay (NRRT). Hemocyte monolayers on glass slides were incubated with 30 mL of 40 mg mL<sup>-1</sup> in DMSO of Neutral Red solution; after 15 min the excess dye was washed out, 30 mL of ASW, and slides were sealed with a coverslip. Control hemocytes were run in parallel. The slides were examined under an optical microscope every 15 min and the percentage of cells showing loss of the dye from lysosomes was calculated. The endpoint of the assay was defined as the time at which 50% of cells showed signs of the lysosomal membrane breaking down (the cytosol is dyed with a red color). The treatments and control were developed by quintuplicates at least. This first response was used to set the concentrations for the other tests.

The phagocytic ability of the hemocytes was assessed by phagocytosis of the neutral red-stained zymosan by hemocyte monolayers. Neutral red-stained zymosan in 0.05 M Tris-HCl buffer (TBS), pH 7.8, containing 2% NaCl was added to each monolayer at a concentration of about 1:30 hemocytes:zymosan in the presence or absence of CNP1 and CNP2 (10 and 50 mg mL<sup>-1</sup>), and allowed to incubate for 60 min. Monolayers were then washed three times with TBS, fixed with Baker's formal calcium (4%, v/v, formaldehyde, 2% NaCl, 1% calcium acetate) for 30 min and mounted in Kaiser's medium for microscopic examination with a Vanox optical microscope. For each slide, the percentage of phagocytic hemocytes was calculated from a minimum of 200 cells. (Canesi et al., 2015; Canesi et al., 2010b). The treatments and controls were developed by eight replicates.

Extracellular generation of superoxide by mussel hemocytes was measured by the reduction of cytochrome c. Hemolymph was extracted into an equal volume of TBS (0.05 M Tris-HCl buffer, pH 7.6, containing 2% NaCl). Aliquots (500  $\mu\text{L}$ ) of hemocyte suspension were incubated with 500  $\mu\text{L}$  of cytochrome c solution (75 mM ferricytochrome c in TBS), with or without CNP1 or CNP2 (final concentration 1 and 50 mg mL<sup>-1</sup>). Cytochrome c in TBS was used as a blank. Samples were read at 550 nm at different times (from 0 to 30 min) and the results expressed as changes in OD per mg protein (Canesi et al., 2015). This assay was developed in triplicate.

#### 2.6. Statistical analysis

Data on biological measurements are given as mean  $\pm$  standard deviation ( $\pm$  SD). Statistical analysis was performed using R version

3.2.2 (Team, 2016). The response variables were lysosomal membrane stability, phagocytosis capacity and ROS production. Generalized linear mixed model GLMM with the observation-level random intercept applied (Zuur et al., 2013) was analyzed using the lme4 package (Bates et al., 2014) in R 3.2.2. Data from phagocytosis capacity and ROS expressed as percentage were transformed by logit transformation prior to analysis. The model included the fixed factors of treatments and concentrations. Data did not violate necessary normality assumptions as tested by visual inspection (quantile–quantile plots) and the Shapiro-Wilk test ( $p > 0.1$ ). Data were graphed using the ggplot2 package (Wickham, 2016).

### 3. Results

#### 3.1. Physicochemical characterization and behavior of CeO<sub>2</sub> NPs in different culture media

The primary size and shape of CNP1 and CNP2 samples were studied by TEM. The average sizes were  $26 \pm 16$  and  $9 \pm 4$  nm for CNP1 and CNP2 respectively (Table 1). CNP1 showed a 43% of particles smaller than 20 nm while CNP2 a 97%. TEM images showed a well-defined shape for CNP1 with respect to CNP2, characterized by their rounded shapes (Table 1). In relation to BET specific surface area, CNP1 had a larger surface-to-volume-ratio with a  $43 \text{ m}^2 \text{ g}^{-1}$  than CNP2 with a value  $18 \text{ m}^2 \text{ g}^{-1}$  (Table 1).

The hydrodynamic radius of CeO<sub>2</sub> NPs or size of agglomerate was studied by DLS over 180 min in ultrapure water and 12 min in AMW and HS from *M. galloprovincialis* (Table 1 and Fig. 1). In ultrapure water the average hydrodynamic radii were 105.8 nm with a PDI: 0.14 and 196.4 nm with a PDI: 0.07 for CNP1 and CNP2 respectively, while in HS the value obtained was 167.8 nm with a PDI: 0.09 and 253.6 nm with a PDI: 0.09 for CNP1 and CNP2, respectively (Table 1). The zeta potential was positive for CNP1 ( $23.6 \pm 0 \text{ mV}$ ) and negative for CNP2 ( $-84.3 \pm 4.31 \text{ mV}$ ) in ultrapure water. The zeta potential changed substantially in ASW and HS, where in ASW, CNP2 showed a substantially negative charge ( $-10 \pm 1.8 \text{ mV}$ ) and CNP1 a positive charge ( $3.2 \pm 0.3 \text{ mV}$ ). In the case of HS, CNP2 showed a substantially greater negative charge ( $-10.2 \pm 0.01 \text{ mV}$ ) than CNP1 ( $-2.6 \pm 0.08 \text{ mV}$ ). CNP1 and CNP2 over 180 min for ultrapure water

and 12 min for HS did not show differences in its hydrodynamic radius when both NPs were suspended in these fluids. However, after 12 min both NPs increased the hydrodynamic radius when they were suspended in artificial marine water showing agglomeration of CeO<sub>2</sub> NPs (Fig. 1).

The Ce<sup>+3</sup>/Ce<sup>+4</sup> ratio measured in ASW Canesi et al. (2017), was higher for CNP2 (0.92) than CNP1 (0.76). These ratios were in line with the results of the higher scavenging activity towards H<sub>2</sub>O<sub>2</sub> in AMW for CNP2 ( $94.31 \pm 3.87\%$ ) than CNP1 ( $76.48 \pm 8.11\%$ ) Sendra et al. (2017a,b,c); see Table 1.

Another difference between the NPs studied was the formation of biocoronas with the surrounding components of HS after 24 h of incubation (Canesi et al., 2017). Only for CNP2 was the formation of a protein corona observed and whose unique component was represented by Cu, Zn-SOD (18 peptides related to Cu, Zn-SOD (K4GX76\_MYTGA) sequence coverage of 84% and high sequest score of 225.82). In contrast, no protein corona was identified for CNP1.

#### 3.2. Effects of CNP1 and CNP2 on the functional parameters of *M. galloprovincialis* hemocytes

##### 3.2.1. Effects on lysosomal membrane stability

LMS showed a dose-response relation from  $10 \text{ mg L}^{-1}$  to  $50 \text{ mg L}^{-1}$  (see Fig. 2(A)). At  $50 \text{ mg L}^{-1}$  statistically relevant biological differences were found in the decrease in LMS; a decrease of 39.02% ( $p < 0.01$ ) in LMS was found in cells exposed to CNP1 with respect to the controls and 49.87% ( $p < 0.01$ ) for cells exposed to CNP2. Furthermore, significant differences were found between CNP1 and CNP2 ( $p < 0.01$ ), where cells exposed to CNP2 decreased the LMS in a 50.9% respect to CNP1 ( $p < 0.01$ ).

##### 3.2.2. Phagocytic activity

Exposure to both CNP1 and CNP2 induced a small but dose-dependent decrease in phagocytic activity of mussel hemocytes. However, at  $50 \text{ mg L}^{-1}$ , decreases in phagocytosis were observed for both CNP1 and CNP2 ( $-21$  and  $-27\%$  respectively;  $p < 0.01$ ). Although there are significant differences between the controls and CNP1, it is biologically meaningless (percentage of phagocytosis activity decreasing less than 20% is irrelevant in this endpoint). However, this response was

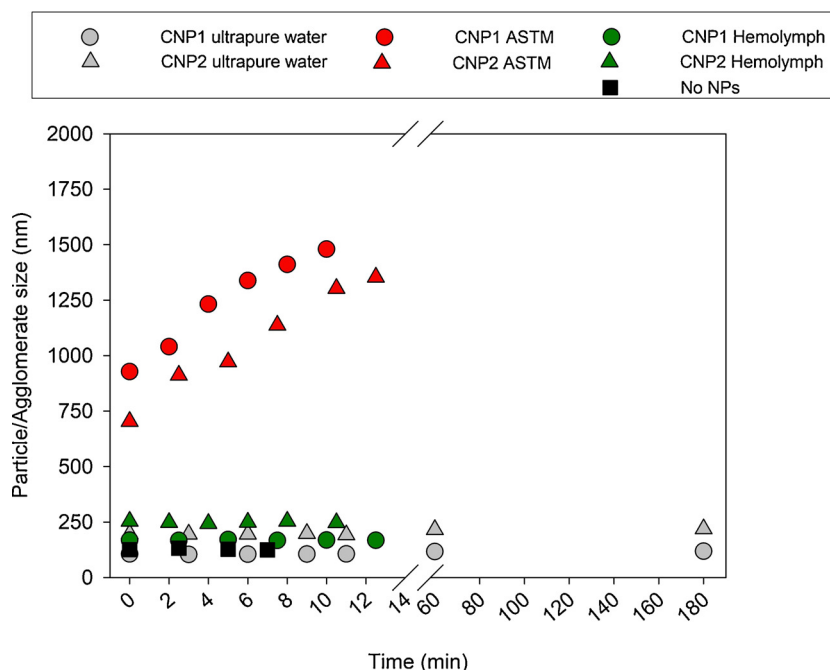


Fig. 1. Size of CNP1 and CNP2 agglomerates in ultrapure water, artificial marine water (ASTM) and hemolymph culture media (filtered by  $0.22 \mu\text{m}$ ) over time.

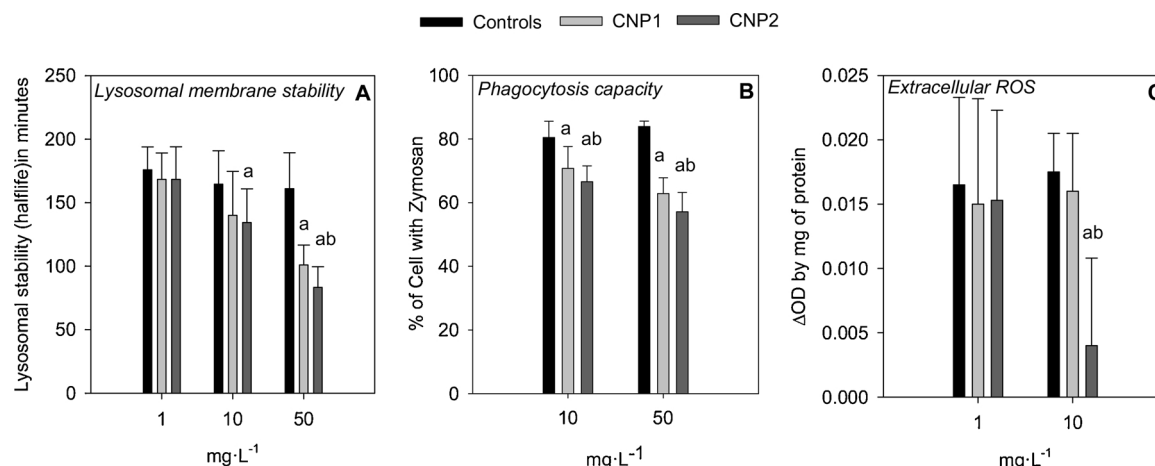


Fig. 2. Toxicological responses measured in hemocyte cells from *M. galloprovincialis*. (A) Lysosomal membrane stability (n = 5–7), (B) phagocytic capacity (n = 8) and extracellular ROS (n = 3–4). Data represent average  $\pm$  SD, a and b letters represent differences with respect to the controls and between CNP1 and CNP2 treatments respectively.

biologically significant in the case of CNP2 with respect to the control and CNP1 ( $p < 0.01$ ); Fig. 2(B).

### 3.2.3. Effects on reactive oxygen species

Extracellular ROS production is shown in Fig. 2(C). Hemocytes exposed to 1 mg L<sup>-1</sup> did not show differences among the controls and CNP1 and CNP2. However, a significant decrease was observed at 10 mg L<sup>-1</sup>. CNP2 decreased extracellular ROS by 77.14% with respect to the controls ( $p < 0.01$ ), whereas CNP1 had an ineffective consequence regarding scavenging ROS.

## 4. Discussion

The CeO<sub>2</sub> NPs tested in this study were shown to be more stable over time in filtered HS than in AMW. Both media showed a large amount of salts; however, some compounds of hemolymph which joined in humoral defense, such as lectins, hydrolytic enzymes and antimicrobial peptides could create a natural soft and/or hard biocorona (Milani et al., 2012), and therefore stabilize NPs in suspension (Canesi et al., 2002b). After the stabilization of NPs with the surrounding fluid, two hypotheses are reached by different authors (Canesi et al., 2017; Canesi et al., 2016a; Hayashi et al., 2016; Hayashi et al., 2013). The first one is that proteins present in the biological serum protect against non-specific adsorption due to lowered membrane adhesion (Lesniak et al., 2013). On the other hand, the second hypothesis is that the biocorona of NPs may have some affinity and activate some membrane receptors and signaling pathways that trigger unwanted responses in bivalves (Canesi et al., 2016b; Garaud et al., 2016; Jimeno-Romero et al., 2016; Katsumiti et al., 2016; Turabekova et al., 2014). The adsorption of protein on the surface of the NPs and therefore biocorona formation depends on: i) physicochemical properties of NPs such as their composition, size (Lundqvist et al., 2008), shape (Deng et al., 2009) and surface charge (Capriotti et al., 2012; Lundqvist et al., 2008; Pozzi et al., 2015; Qiu et al., 2010) and ii) biological environment such as type of plasma, incubation time, temperature, pH and the physiological state of the plasma (Hajipour et al., 2014; Mahmoudi et al., 2013; Pozzi et al., 2015; Tenzer et al., 2013). The surface curvature has an important role in protein adsorption and corona composition (Lundqvist et al., 2008). Mathematical models and experimental studies have revealed that adsorbed proteins on the curved surface of NPs undergo less conformational changes than proteins adsorbed on flat surfaces of the same material (Mahmoudi et al., 2011; Rahman et al., 2013). Moreover, the selective adsorption and binding of proteins on NPs with different shapes was demonstrated in a study with TiO<sub>2</sub> NPs,

spherical TiO<sub>2</sub> NPs were unique in displaying apolipoprotein D and clustering, whereas no such proteins were identified on rod- or tube-shaped TiO<sub>2</sub>NPs (Deng et al., 2009). This is in agreement with the CeO<sub>2</sub> NPs employed in this study where the only NPs with rounded shape (CNP2) formed Cu, Zn-SOD protein corona (Canesi et al., 2017).

Protein adsorption to the NPs' surface may mediate the uptake via receptor-mediated endocytosis (Alkilany and Murphy, 2010; Conner and Schmid, 2003). The uptake of nanoparticles by cells can be viewed as a two-step process: first a binding step on the cell membrane and second the internalization step (Wilhelm et al., 2003). Some factors might be important in the uptake NPs into cells; one of the uptake factors is the cell surface coating and charge of nanoparticles. Positive or negative zeta potential has been shown to be dependent on the synthesis process of CeO<sub>2</sub> NPs. According to Patil et al. (2007) the CeO<sub>2</sub> NPs synthesized in pH 1 buffer showed positive zeta potential, while pH 13 buffer produced particles with negative zeta potential independently of the synthesis methods used for their fabrication (Patil et al., 2007). These results are in line with the present work. CNP1 at 5 mg L<sup>-1</sup> in ultrapure water had a pH of 4.3 and a zeta potential of  $23.6 \pm 8.3$  mV, while the pH of CNP2 was 8.5 with a zeta potential of  $-84 \pm 4.3$  mV (Sendra et al., 2017c). These findings consequently support the premise that the pH of the buffer for the NPs during manufacture is a key factor governing the particle's zeta potential. The zeta potential of NPs plays an important role in biocorona formation in HS of bivalves (Canesi et al., 2017; Canesi et al., 2016a). The recent finding of Canesi et al. (2017) showed that two types of metallic oxide NPs such as TiO<sub>2</sub> NPs and CeO<sub>2</sub> NPs (CNP2) with negative zeta potential in HS were able to form the same hard protein corona of Cu, Zn-SOD. However, CNP1 (CeO<sub>2</sub> NPs) with minimal values of zeta potential did not show any peptides when it was analyzed.

Our results further showed higher changes in the biomarkers of stress (LMS) and immunological parameters (phagocytosis capacity and extracellular ROS generation) of hemocyte cells when the CNP2 treatment was tested (with negative zeta potential, rounded shape and protein corona formation) compared to hemocytes exposed to CNP1 (almost neutral zeta potential, well-faceted shape and no protein corona detected). The most of study relate the toxicity with positive zeta potential (Pang et al., 2016). In this study, the authors found that AgNPs with positive values of zeta potential; +46.5 mV, induced the highest cytotoxicity and DNA fragmentation in Hepa1c1c7. In addition, these authors showed the highest damage to the nucleus of liver cells. Cho et al. (2009) found that Au NPs with a positive charge were the most internalized NPs followed by negative nanoparticles and in the last place neutral nanoparticles in breast cancer cells (Cho et al., 2009).

There has been evidence of the uptake of negatively charged particles despite the unfavorable interaction between the particles and the negatively charged cell membrane. These authors examined the role of surface charge in the internalization of Au NPs, and the negatively charged nanoparticles were internalized through nonspecific binding and clustering of the particles on cationic sites on the plasma membrane (that are relatively scarcer than negatively charged domains). Later, the mechanism which has the greatest efficiency in cell-membrane penetration and cellular internalization is the endocytosis positively charged particles. They form the primary platform as synthetic carriers for drug and gene delivery (Cho et al., 2009). However, a study has reported that there are some positively charged regions on the cell surface such as cationized hemeundecapeptide (cHUP) and cationized ferritin on cell surface. This could facilitate the uptake of negatively charged nanoparticles (Ghinea and Simionescu, 1985).

Other properties of NPs that can influence the health status of the cell are the size and shape of NPs in the aqueous media without taking into account the biocorona formation of CNP2. In this work we found that rounded NPs with negative zeta potential (CNP2) provoked greater changes in the biomarkers of stress and immunological parameters than the well-faceted surface NPs with almost neutral zeta potential (CNP1) (see TEM image, Fig. 2). These findings are in accordance with previous work which demonstrated that rounded NPs could be internalized 500% more than rod-shape NPs due to the greater membrane wrapping time required for the elongated particles (Chithrani and Chan, 2007; Chithrani et al., 2006). Nanoparticles between 2 and 100 nm size range were found to alter signaling processes including the signaling pathways of death receptors (Jiang et al., 2008). In many studies, results showed the greatest effects on biological functions and the bioaccumulation of small size metallic NPs rather than larger agglomerates (Coradeghini et al., 2013; Garcia-Negrete et al., 2013; Katsumiti et al., 2016; Liu et al., 2014; Tedesco et al., 2010; Tedesco et al., 2008). In this study, no relation between stress and effect on immunological parameters and smaller NPs agglomerates in HS (CNP1) were found, therefore we can conclude that under these test conditions the main factors of CeO<sub>2</sub> NPs which disturb the health cell status were the negative zeta potential, Cu, Zn-SOD biocorona and a rounded shape for the different mechanisms of NPs adsorption onto cells and uptake previously described.

Once NPs are internalized by cells, they are expected to be recognized as foreign agents and stored in the lysosomes for digestion (Allen and Moore, 2004; Moore et al., 2006). Lack of LMS was reported for the CeO<sub>2</sub> NPs tested. This lack of LMS has been noted for other nanoparticles of different composition such as C60 fullerene, TiO<sub>2</sub>, SiO<sub>2</sub> and nano-carbon black when exposed to bivalve hemocytes (Betti et al., 2006; Canesi et al., 2008; Canesi and Corsi, 2016). The lack of LMS may be related, as showed by other authors, with lysozyme release (Canesi et al., 2008; Canesi et al., 2016b; Canesi et al., 2010b). This finding should be examined more closely using biomarkers of inflammation such as cyclooxygenase activity, cytokine release or the production of nitrous oxide (Gagné et al., 2006).

Down-regulation in cell signaling is related to a decrease in phagocytosis capacity as a defense mechanism, which was observed in the hemocyte cells treated with CNP2. Phagocytosis is the main defense mechanism for the bivalves, therefore reduced phagocytosis may be a detrimental effect producing an alteration in food ingestion, energy assimilation processes, ability to remove foreign bodies, and overall viability of cells (Abbott Chalew et al., 2012; Cheng, 1996). The processes of phagocytosis are regulated by activation of MAPK pathways (Aam and Fonnum, 2007; Chin et al., 1998). Some studies indicate that a decrease in the phosphorylation stage of all MAPK members (ERK, p38, JNKs) and PKC can provoke a down-regulation in cell signaling, and therefore an immunodepression of hemocyte cells (Betti et al., 2006; Canesi et al., 2006). An alteration in the phagocytosis capacity of bivalve hemocytes when they are exposed to NPs has been demonstrated by many authors over the last years (Abbott Chalew et al., 2012;

Marisa et al., 2015). So any change in MAPK may affect not only phagocytosis capacity, but apoptosis, transcription, translation and nucleic acids and cytoskeleton functions (Boya and Kroemer, 2008; Cheng and Sullivan, 1984; Fries and Tripp, 1980; Grundy et al., 1996; Yang et al., 2003).

ROS production controls phagocytosis capacity and it regulates the presence of foreign bodies inside the cells (Canesi et al., 2005; Canesi et al., 2012). Therefore, a deregulation of ROS can affect the innate immune system. Another cause of ROS decrease in this research might be due to the mimetic activity of CeO<sub>2</sub> NPs with antioxidant enzymes (ratio Ce<sup>+3</sup>/Ce<sup>+4</sup> on NPs surface), therefore it may reduce the percentage of ROS levels in treatments with CeO<sub>2</sub> NPs.

## 5. Conclusions

In conclusion, CeO<sub>2</sub> NPs at tested concentrations provoked changes in a battery of functional parameters (LMS, ROS and phagocytosis capacity) in hemocytes of *Mytilus galloprovincialis* and led to a down-regulation of immune systems as evidenced by the loss of LMS and a decrease in the phagocytosis capacity of the cells. The overall responses studied in these in vitro experiments carried out in HS showed a dose-response trend. Smaller agglomerates of NPs were not related to higher shifts in the biomarkers of stress and immunological parameters, but negative zeta potential, the rounded shape of CNP2 and protein corona formation with respect to almost neutral zeta potential, well-faceted surface and no biocorona formation of CNP1 showed the importance of intrinsic characteristics of NPs and extrinsic properties of the culture media in the negative effects of CeO<sub>2</sub> NPs to marine mussel hemocytes. This information will allow improving the risk assessment of CeO<sub>2</sub> NPs in hemocytes of mussels. Therefore, the study of primary, secondary NPs characteristics and interaction between NPs with biological fluids is necessary to understand its bioavailability, behavior and toxicity at cellular level. Furthermore, the authors suggest a deeply study about colloidal forces between NPs and cells, membrane, DNA and proteins to understand the interaction and interface between NPs-cells.

## Acknowledgments

This research has been funded by the Junta de Andalucía (PE2011-RNM-7812 project and FQM-110 group) and the Spanish National Research Plan (CTM2012-38720-C03-03, Project MINECO/FEDER MAT2013-40823-R and CTM2016-75908-R). We are also grateful to IFAPA research center specially Catalina Fernandez for the support in measuring DLS and the SCICYT of Cadiz University (UCA) for the use of its Electron Microscopy division facilities.

## References

- ASTM, 1975. Standard Specification for Substitute Ocean Water. American Standard for Testing and Materials (Designation D 1141-75).
- Aam, B.B., Fonnum, F., 2007. ROS scavenging effects of organic extract of diesel exhaust particles on human neutrophil granulocytes and rat alveolar macrophages. *Toxicology* 230, 207–218.
- Abbott Chalew, T.E., Galloway, J.F., Graczyk, T.K., 2012. Pilot study on effects of nanoparticle exposure on *Crassostrea virginica* hemocyte phagocytosis. *Mar. Pollut. Bull.* 64, 2251–2253.
- Afratis, N., Gialeli, C., Nikitovic, D., Tsegenidis, T., Karousou, E., Theocharis, A.D., Pavão, M.S., Tzanakakis, G.N., Karamanos, N.K., 2012. Glycosaminoglycans: key players in cancer cell biology and treatment. *FEBS J.* 279, 1177–1197.
- Alkilany, A.M., Murphy, C.J., 2010. Toxicity and cellular uptake of gold nanoparticles: what we have learned so far? *J. Nanopart. Res.* 12, 2313–2333.
- Allen, J.I., Moore, M.N., 2004. Environmental prognostics: is the current use of biomarkers appropriate for environmental risk evaluation? *Mar. Environ. Res.* 58, 227–232.
- Asghari, S., Johari, S.A., Lee, J.H., Kim, Y.S., Jeon, Y.B., Choi, H.J., Moon, M.C., Yu, I.J., 2012. Toxicity of various silver nanoparticles compared to silver ions in *Daphnia magna*. *J. Nanobiotechnol.* 10, 14.
- Baker, T.J., Tyler, C.R., Galloway, T.S., 2014. Impacts of metal and metal oxide nanoparticles on marine organisms. *Environ. Pollut.* 186, 257–271.
- Bates, D., Maechler, M., Bolker, B., Walker, S., 2014. *lme4: Linear Mixed-effects Models Using Eigen and S4*. R package version 1.

- Betti, M., Ciacci, C., Lorusso, L.C., Canonico, B., Falcioni, T., Gallo, G., Canesi, L., 2006. Effects of tumour necrosis factor  $\alpha$  (TNF $\alpha$ ) on Mytilus haemocytes: role of stress-activated mitogen-activated protein kinases (MAPKs). *Biol. Cell* 98, 233–244.
- Bouris, P., Skandalis, S.S., Piperigkou, Z., Afratis, N., Karamanou, K., Aletras, A.J., Moustakas, A., Theocharis, A.D., Karamanos, N.K., 2015. Estrogen receptor alpha mediates epithelial to mesenchymal transition, expression of specific matrix effectors and functional properties of breast cancer cells. *Matrix Biol.* 43, 42–60.
- Boya, P., Kroemer, G., 2008. Lysosomal membrane permeabilization in cell death. *Oncogene* 27, 6434–6451.
- Buffet, P.-E., Tankoua, O.F., Pan, J.-F., Berhanu, D., Herrenknecht, C., Poirier, L., Amiard-Triquet, C., Amiard, J.-C., Bérard, J.-B., Risso, C., 2011. Behavioural and biochemical responses of two marine invertebrates *Scrobicularia plana* and *Hediste diversicolor* to copper oxide nanoparticles. *Chemosphere* 84, 166–174.
- Canesi, L., Corsi, I., 2016. Effects of nanomaterials on marine invertebrates. *Sci. Total Environ.* 565, 933–940.
- Canesi, L., Procházová, P., 2013. The invertebrate immune system as a model for investigating the environmental impact of nanoparticles: nanoparticles and the immune system. *Saf. Effects* 7, 91–112.
- Canesi, L., Gallo, G., Gavioli, M., Pruzzo, C., 2002a. Bacteria–hemocyte interactions and phagocytosis in marine bivalves. *Microsc. Res. Tech.* 57, 469–476.
- Canesi, L., Scarpato, A., Betti, M., Ciacci, C., Pruzzo, C., Gallo, G., 2002b. Bacterial killing by *Mytilus* hemocyte monolayers as a model for investigating the signaling pathways involved in mussel immune defence. *Mar. Environ. Res.* 54, 547–551.
- Canesi, L., Ciacci, C., Betti, M., Scarpato, A., Citterio, B., Pruzzo, C., Gallo, G., 2003. Effects of PCB congeners on the immune function of *Mytilus* hemocytes: alterations of tyrosine kinase-mediated cell signalling. *Aquat. Toxicol.* 63, 293–306.
- Canesi, L., Betti, M., Ciacci, C., Lorusso, L.C., Gallo, G., Pruzzo, C., 2005. Interactions between *Mytilus* haemocytes and different strains of *Escherichia coli* and *Vibrio cholerae* O1 El Tor: role of kinase-mediated signalling. *Cell. Microbiol.* 7, 667–674.
- Canesi, L., Betti, M., Ciacci, C., Lorusso, L., Pruzzo, C., Gallo, G., 2006. Cell signalling in the immune response of mussel hemocytes. *Invertebrate Surviv. J.* 3, 40–49.
- Canesi, L., Ciacci, C., Lorusso, L.C., Betti, M., Gallo, G., Pojana, G., Marcomini, A., 2007. Effects of Triclosan on *Mytilus galloprovincialis* hemocyte function and digestive gland enzyme activities: possible modes of action on non target organisms. *Comp. Biochem. Physiol. Part C Toxicol. Pharmacol.* 145, 464–472.
- Canesi, L., Ciacci, C., Betti, M., Fabbri, R., Canonico, B., Fantinati, A., Marcomini, A., Pojana, G., 2008. Immunotoxicity of carbon black nanoparticles to blue mussel hemocytes. *Environ. Int.* 34, 1114–1119.
- Canesi, L., Ciacci, C., Vallotto, D., Gallo, G., Marcomini, A., Pojana, G., 2010a. In vitro effects of suspensions of selected nanoparticles (C60 fullerene, TiO<sub>2</sub>, SiO<sub>2</sub>) on *Mytilus* hemocytes. *Aquat. Toxicol.* 96, 151–158.
- Canesi, L., Fabbri, R., Gallo, G., Vallotto, D., Marcomini, A., Pojana, G., 2010b. Biomarkers in *Mytilus galloprovincialis* exposed to suspensions of selected nanoparticles (Nano carbon black, C60 fullerene, Nano-TiO<sub>2</sub>, Nano-SiO<sub>2</sub>). *Aquat. Toxicol.* 100, 168–177.
- Canesi, L., Ciacci, C., Fabbri, R., Marcomini, A., Pojana, G., Gallo, G., 2012. Bivalve molluscs as a unique target group for nanoparticle toxicity. *Mar. Environ. Res.* 76, 16–21.
- Canesi, L., Frenzilli, G., Balbi, T., Bernardeschi, M., Ciacci, C., Corsolini, S., Della Torre, C., Fabbri, R., Faleri, C., Focardi, S., 2014. Interactive effects of n-TiO<sub>2</sub> and 2, 3, 7, 8-TCDD on the marine bivalve *Mytilus galloprovincialis*. *Aquat. Toxicol.* 153, 53–65.
- Canesi, L., Ciacci, C., Bergami, E., Monopoli, M., Dawson, K., Papa, S., Canonico, B., Corsi, I., 2015. Evidence for immunomodulation and apoptotic processes induced by cationic polystyrene nanoparticles in the hemocytes of the marine bivalve *Mytilus*. *Mar. Environ. Res.* 111, 34–40.
- Canesi, L., Ciacci, C., Balbi, T., 2016a. Invertebrate models for investigating the impact of nanomaterials on innate immunity: the example of the marine mussel *Mytilus* spp. *Curr. Bionanotechnol.* 2, 77–83.
- Canesi, L., Ciacci, C., Fabbri, R., Balbi, T., Salis, A., Damonte, G., Cortese, K., Caratto, V., Monopoli, M.P., Dawson, K., 2016b. Interactions of cationic polystyrene nanoparticles with marine bivalve hemocytes in a physiological environment: role of soluble hemolymph proteins. *Environ. Res.* 150, 73–81.
- Canesi, L., Balbi, T., Fabbri, R., Salis, A., Damonte, G., Volland, M., Blasco, J., 2017. Biomolecular coronas in invertebrate species: implications in the environmental impact of nanoparticles. *NanoImpact* 8, 89–98.
- Capriotti, A.L., Caracciolo, G., Cavaliere, C., Foglia, P., Pozzi, D., Samperi, R., Laganà, A., 2012. Do plasma proteins distinguish between liposomes of varying charge density? *J. Proteomics* 75, 1924–1932.
- Celardo, I., Pedersen, J.Z., Traversa, E., Ghibelli, L., 2011. Pharmacological potential of cerium oxide nanoparticles. *Nanoscale* 3, 1411–1420.
- Cheng, T.C., Sullivan, J.T., 1984. Effects of heavy metals on phagocytosis by molluscan hemocytes. *Mar. Environ. Res.* 14, 305–315.
- Cheng, T.C., 1996. Hemocytes: forms and functions. *The Eastern Oyster Crassostrea Virginica*, vol. 1. pp. 75–93.
- Chin, B.Y., Choi, M.E., Burdick, M.D., Strieter, R.M., Risby, T.H., Choi, A.M., 1998. Induction of apoptosis by particulate matter: role of TNF- $\alpha$  and MAPK. *Am. J. Physiol.-Lung Cell. Mol. Physiol.* 275, L942–L949.
- Chithrani, B.D., Chan, W.C., 2007. Elucidating the mechanism of cellular uptake and removal of protein-coated gold nanoparticles of different sizes and shapes. *Nano Lett.* 7, 1542–1550.
- Chithrani, B.D., Ghazani, A.A., Chan, W.C., 2006. Determining the size and shape dependence of gold nanoparticle uptake into mammalian cells. *Nano Lett.* 6, 662–668.
- Cho, E.C., Xie, J., Wurm, P.A., Xia, Y., 2009. Understanding the role of surface charges in cellular adsorption versus internalization by selectively removing gold nanoparticles on the cell surface with a 12/KI etchant. *Nano Lett.* 9, 1080–1084.
- Ciacci, C., Canonico, B., Bilaničová, D., Fabbri, R., Cortese, K., Gallo, G., Marcomini, A., Pojana, G., Canesi, L., 2012. Immunomodulation by different types of N-Oxides in the hemocytes of the marine bivalve *Mytilus galloprovincialis*. *PLoS One* 7, e36937.
- Clément, L., Hurel, C., Marmier, N., 2013. Toxicity of TiO<sub>2</sub> nanoparticles to cladocerans, algae, rotifers and plants—effects of size and crystalline structure. *Chemosphere* 90, 1083–1090.
- Conner, S.D., Schmid, S.L., 2003. Regulated portals of entry into the cell. *Nature* 422, 37–44.
- Coradeghini, R., Gioria, S., García, C.P., Nativo, P., Franchini, F., Gilliland, D., Ponti, J., Rossi, F., 2013. Size-dependent toxicity and cell interaction mechanisms of gold nanoparticles on mouse fibroblasts. *Toxicol. Lett.* 217, 205–216.
- Croteau, M.-N., Dybowska, A.D., Luoma, S.N., Valsami-Jones, E., 2011a. A novel approach reveals that zinc oxide nanoparticles are bioavailable and toxic after dietary exposures. *Nanotoxicology* 5, 79–90.
- Croteau, M.-N., Misra, S.K., Luoma, S.N., Valsami-Jones, E., 2011b. Silver bioaccumulation dynamics in a freshwater invertebrate after aqueous and dietary exposures to nanosized and ionic Ag. *Environ. Sci. Technol.* 45, 6600–6607.
- Deng, Z.J., Mortimer, G., Schiller, T., Musumeci, A., Martin, D., Minchin, R.F., 2009. Differential plasma protein binding to metal oxide nanoparticles. *Nanotechnology* 20.
- Fries, C., Tripp, M., 1980. Depression of phagocytosis in *Mercenaria* following chemical stress. *Dev. Comp. Immunol.* 4, 233–244.
- Gagné, F., Blaise, C., Fournier, M., Hansen, P., 2006. Effects of selected pharmaceutical products on phagocytic activity in *Elliptio complanata* mussels. *Comp. Biochem. Physiol. Part C Toxicol. Pharmacol.* 143, 179–186.
- Gagné, F., Auclair, J., Turcotte, P., Fournier, M., Gagnon, C., Sauvé, S., Blaise, C., 2008. Ecotoxicity of CdTe quantum dots to freshwater mussels: impacts on immune system, oxidative stress and genotoxicity. *Aquat. Toxicol.* 86, 333–340.
- Garaud, M., Auffan, M., Devin, S., Felten, V., Pagnout, C., Pain-Devin, S., Proux, O., Rodius, F., Sohm, B., Giamberini, L., 2016. Integrated assessment of ceria nanoparticle impacts on the freshwater bivalve *Dreissena polymorpha*. *Nanotoxicology* 10, 935–944.
- García-Negrete, C., Blasco, J., Volland, M., Rojas, T.C., Hampel, M., Lapresta-Fernández, A., De Haro, M.J., Soto, M., Fernández, A., 2013. Behaviour of Au-citrate nanoparticles in seawater and accumulation in bivalves at environmentally relevant concentrations. *Environ. Pollut.* 174, 134–141.
- Ghinea, N., Simionescu, N., 1985. Anionized and cationized hemeundecapeptides as probes for cell surface charge and permeability studies: differentiated labeling of endothelial plasmalemmal vesicles. *J. Cell Biol.* 100, 606–612.
- Gialeli, C., Theocharis, A.D., Karamanos, N.K., 2011. Roles of matrix metalloproteinases in cancer progression and their pharmacological targeting. *FEBS J.* 278, 16–27.
- Gomes, T., Pinheiro, J.P., Cancio, L., Pereira, C.G., Cardoso, C., Bebianno, M.J., 2011. Effects of copper nanoparticles exposure in the mussel *Mytilus galloprovincialis*. *Environ. Sci. Technol.* 45, 9356–9362.
- Gomes, T., Araújo, O., Pereira, R., Almeida, A.C., Cravo, A., Bebianno, M.J., 2013. Genotoxicity of copper oxide and silver nanoparticles in the mussel *Mytilus galloprovincialis*. *Mar. Environ. Res.* 84, 51–59.
- Gottschalk, F., Lassen, C., Kjoelholm, J., Christensen, F., Nowack, B., 2015. Modeling flows and concentrations of nine engineered nanomaterials in the danish environment. *Int. J. Environ. Res. Public Health* 12, 5581–5602.
- Grundy, M., Moore, M., Howell, S., Ratcliffe, N., 1996. Phagocytic reduction and effects on lysosomal membranes by polycyclic aromatic hydrocarbons, in hemocytes of *Mytilus edulis*. *Aquat. Toxicol.* 34, 273–290.
- Hadjimetriou, M., Kostarelou, K., 2017. Nanomedicine: evolution of the nanoparticle corona. *Nat Nano* 12, 288–290.
- Hajipour, M.J., Laurent, S., Aghaie, A., Rezaee, F., Mahmoudi, M., 2014. Personalized protein coronas: a key factor at the nanobiointerface. *Biomater. Sci.* 2, 1210–1221.
- Hayashi, Y., Miclaus, T., Scavenius, C., Kwiatkowska, K., Sobota, A., Engelmann, P., Scott-Fordsmand, J.J., Enghild, J.J., Sutherland, D.S., 2013. Species differences take shape at nanoparticles: protein corona made of the native repertoire assists cellular interaction. *Environ. Sci. Technol.* 47, 14367–14375.
- Hayashi, Y., Miclaus, T., Engelmann, P., Autrup, H., Sutherland, D.S., Scott-Fordsmand, J.J., 2016. Nanosilver pathophysiology in earthworms: transcriptional profiling of secretory proteins and the implication for the protein corona. *Nanotoxicology* 10, 303–311.
- Izu, N., Shin, W., Matsubara, I., Murayama, N., 2004. Development of resistive oxygen sensors based on cerium oxide thick film. *J. Electroceram.* 13, 703–706.
- Jiang, W., Kim, B.Y., Rutka, J.T., Chan, W.C., 2008. Nanoparticle-mediated cellular response is size-dependent. *Nat. Nanotechnol.* 3, 145–150.
- Jimeno-Romero, A., Oron, M., Cajaraville, M., Soto, M., Marigómez, I., 2016. Nanoparticle size and combined toxicity of TiO<sub>2</sub> and DSLS (surfactant) contribute to lysosomal responses in digestive cells of mussels exposed to TiO<sub>2</sub> nanoparticles. *Nanotoxicology* 10, 1168–1176.
- Katsumiti, A., Gilliland, D., Arostegui, I., Cajaraville, M.P., 2015. Mechanisms of toxicity of ag nanoparticles in comparison to bulk and ionic ag on mussel hemocytes and gill cells. *PLoS One* 10, e0129039.
- Katsumiti, A., Arostegui, I., Oron, M., Gilliland, D., Valsami-Jones, E., Cajaraville, M.P., 2016. Cytotoxicity of Au, ZnO and SiO<sub>2</sub> NPs using in vitro assays with mussel hemocytes and gill cells: relevance of size, shape and additives. *Nanotoxicology* 10, 185–193.
- Lesniak, A., Salvati, A., Santos-Martinez, M.J., Radomski, M.W., Dawson, K.A., Åberg, C., 2013. Nanoparticle adhesion to the cell membrane and its effect on nanoparticle uptake efficiency. *J. Am. Chem. Soc.* 135, 1438–1444.
- Liu, Z., Wu, Y., Guo, Z., Liu, Y., Shen, Y., Zhou, P., Lu, X., 2014. Effects of internalized gold nanoparticles with respect to cytotoxicity and invasion activity in lung cancer cells. *PLoS One* 9, e99175.
- Lundqvist, M., Stigler, J., Elia, G., Lynch, I., Cedervall, T., Dawson, K.A., 2008. Nanoparticle size and surface properties determine the protein corona with possible

- implications for biological impacts. *Proc. Natl. Acad. Sci. U. S. A.* 105, 14265–14270.
- Lynch, I., Dawson, K.A., 2008. Protein-nanoparticle interactions. *Nano Today* 3, 40–47.
- Mahmoudi, M., Lynch, I., Ejtehadi, M.R., Monopoli, M.P., Bombelli, F.B., Laurent, S., 2011. Protein-nanoparticle interactions: opportunities and challenges. *Chem. Rev.* 111, 5610–5637.
- Mahmoudi, M., Abdelmonem, A.M., Behzadi, S., Clement, J.H., Dutz, S., Ejtehadi, M.R., Hartmann, R., Kantner, K., Linne, U., Maffre, P., 2013. Temperature: the ignored factor at the nanobio interface. *ACS Nano* 7, 6555–6562.
- Marisa, I., Marin, M.G., Caicci, F., Franceschinis, E., Martucci, A., Matozzo, V., 2015. In vitro exposure of haemocytes of the clam *Ruditapes philippinarum* to titanium dioxide (TiO<sub>2</sub>) nanoparticles: nanoparticle characterisation, effects on phagocytic activity and internalisation of nanoparticles into haemocytes. *Mar. Environ. Res.* 103, 11–17.
- Milani, S., Baldelli Bombelli, F., Pitek, A.S., Dawson, K.A., Rädler, J., 2012. Reversible versus irreversible binding of transferrin to polystyrene nanoparticles: soft and hard Corona. *ACS Nano* 6, 2532–2541.
- Moore, M.N., Allen, J.I., McVeigh, A., 2006. Environmental prognostics: an integrated model supporting lysosomal stress responses as predictive biomarkers of animal health status. *Mar. Environ. Res.* 61, 278–304.
- Moore, M.N., 2006. Do nanoparticles present ecotoxicological risks for the health of the aquatic environment? *Environ. Int.* 32, 967–976.
- Murray, E.P., Tsai, T., Barnett, S., 1999. A direct-methane fuel cell with a ceria-based anode. *Nature* 400, 649–651.
- Neagu, M., Piperigkou, Z., Karamanou, K., Engin, A.B., Docea, A.O., Constantin, C., Negrei, C., Nikitovic, D., Tsatsakis, A., 2017. Protein bio-corona: critical issue in immune nanotoxicology. *Arch. Toxicol.* 91, 1031–1048.
- Nel, A.E., Mädlar, L., Velegol, D., Xia, T., Hoek, E.M., Somasundaran, P., Klaessig, F., Castranova, V., Thompson, M., 2009. Understanding biophysicochemical interactions at the nano-bio interface. *Nat. Mater.* 8, 543–557.
- Nguyen Quang, K., Byung Sun, K., Dao Ngoc, N., Luu Minh, D., 2011. UV Absorption by Cerium Oxide Nanoparticles/epoxy Composite Thin Films.
- Oliveira-Filho, E.C., Sousa Filho, J., Novais, L.A., Peterle, W.S., Azevedo, R.B., Grisolia, C.K., 2016. Effects of  $\gamma$ -Fe<sub>2</sub>O<sub>3</sub> nanoparticles on the survival and reproduction of *Biomphalaria glabrata* (Say, 1818) and their elimination from this benthic aquatic snail. *Environ. Sci. Pollut. Res. Int.* 23, 18362–18368.
- Pang, C., Brunelli, A., Zhu, C., Hristozov, D., Liu, Y., Semenzin, E., Wang, W., Tao, W., Liang, J., Marcomini, A., Chen, C., Zhao, B., 2016. Demonstrating approaches to chemically modify the surface of Ag nanoparticles in order to influence their cytotoxicity and biodistribution after single dose acute intravenous administration. *Nanotoxicology* 10, 129–139.
- Patil, S., Sandberg, A., Heckert, E., Self, W., Seal, S., 2007. Protein adsorption and cellular uptake of cerium oxide nanoparticles as a function of zeta potential. *Biomaterials* 28, 4600–4607.
- Pozzi, D., Caracciolo, G., Capriotti, A.L., Cavaliere, C., La Barbera, G., Anchordoquy, T.J., Laganà, A., 2015. Surface chemistry and serum type both determine the nanoparticle-protein corona. *J. Proteomics* 119, 209–217.
- Pruzzo, C., Gallo, G., Canesi, L., 2005. Persistence of vibrios in marine bivalves: the role of interactions with haemolymph components. *Environ. Microbiol.* 7, 761–772.
- Qiu, Y., Liu, Y., Wang, L., Xu, L., Bai, R., Ji, Y., Wu, X., Zhao, Y., Li, Y., Chen, C., 2010. Surface chemistry and aspect ratio mediated cellular uptake of Au nanorods. *Biomaterials* 31, 7606–7619.
- Rahman, M., Laurent, S., Tawil, N., Yahia, L., Mahmoudi, M., 2013. Protein-nanoparticle Interactions. Springer.
- Rodea-Palomares, I., Boltos, K., Fernández-Piñas, F., Leganés, F., García-Calvo, E., Santiago, J., Rosal, R., 2011. Physicochemical characterization and ecotoxicological assessment of CeO<sub>2</sub> nanoparticles using two aquatic microorganisms. *Toxicol. Sci.* 119, 135–145.
- Selvan, V.A.M., Anand, R., Udayakumar, M., 2009. Effects of cerium oxide nanoparticle addition in diesel and diesel-biodiesel-ethanol blends on the performance and emission characteristics of a CI engine. *J. Eng. Appl. Sci.* 4, 1819–6608.
- Sendra, M., Pintado-Herrera, M., Aguirre-Martínez, G., Moreno-Garrido, I., Martín-Díaz, L., Lara-Martín, P., Blasco, J., 2017a. Are the TiO<sub>2</sub> NPs a Trojan horse for personal care products (PCPs) in the clam *Ruditapes philippinarum*? *Chemosphere* 185, 192–204.
- Sendra, M., Yeste, M.P., Gatica, J.M., Moreno-Garrido, I., Blasco, J., 2017b. Direct and indirect effects of silver nanoparticles on freshwater and marine microalgae (*Chlamydomonas reinhardtii* and *Phaeodactylum tricornutum*). *Chemosphere* 179, 279–289.
- Sendra, M., Yeste, P., Moreno-Garrido, I., Gatica, J., Blasco, J., 2017c. CeO<sub>2</sub> NPs, toxic or protective to phytoplankton? Charge of nanoparticles and cell wall as factors which cause changes in cell complexity. *Sci. Total Environ.* 590, 304–315.
- Shi, W., Han, Y., Guo, C., Zhao, X., Liu, S., Su, W., Zha, S., Wang, Y., Liu, G., 2017. Immunotoxicity of nanoparticle nTiO<sub>2</sub> to a commercial marine bivalve species, *Tegillarca granosa*. *Fish Shellfish Immunol.* 66, 300–306.
- Team, R.C., 2016. A Language and Environment for Statistical Computing. R Foundation for statistical computing, 2015, Vienna, Austria.
- Tedesco, S., Doyle, H., Redmond, G., Sheehan, D., 2008. Gold nanoparticles and oxidative stress in *Mytilus edulis*. *Mar. Environ. Res.* 66, 131–133.
- Tedesco, S., Doyle, H., Blasco, J., Redmond, G., Sheehan, D., 2010. Oxidative stress and toxicity of gold nanoparticles in *Mytilus edulis*. *Aquat. Toxicol.* 100, 178–186.
- Tenzer, S., Docter, D., Kuharev, J., Musyanovych, A., Fetz, V., Hecht, R., Schlenk, F., Fischer, D., Kiouptsi, K., Reinhardt, C., 2013. Rapid formation of plasma protein corona critically affects nanoparticle pathophysiology. *Nat. Nanotechnol.* 8, 772–781.
- Teske, S.S., Detweiler, C.S., 2015. The biomechanisms of metal and metal-oxide nanoparticles' interactions with cells. *Int. J. Environ. Res. Public Health* 12, 1112–1134.
- Thit, A., Huggins, K., Selck, H., Baun, A., 2017. Acute toxicity of copper oxide nanoparticles to *Daphnia magna* under different test conditions. *Toxicol. Environ. Chem.* 99, 665–679.
- Turabekova, M., Rasulev, B., Theodore, M., Jackman, J., Leszczynska, D., Leszczynski, J., 2014. Immunotoxicity of nanoparticles: a computational study suggests that CNTs and C 60 fullerenes might be recognized as pathogens by Toll-like receptors. *Nanoscale* 6, 3488–3495.
- Wang, Y., Hu, M., Li, Q., Li, J., Lin, D., Lu, W., 2014. Immune toxicity of TiO<sub>2</sub> under hypoxia in the green-lipped mussel *Perna viridis* based on flow cytometric analysis of hemocyte parameters. *Sci. Total Environ.* 470, 791–799.
- Wickham, H., 2016. *Ggplot2: Elegant Graphics for Data Analysis*. Springer.
- Wilhelm, C., Billotey, C., Roger, J., Pons, J., Bacri, J.-C., Gazeau, F., 2003. Intracellular uptake of anionic superparamagnetic nanoparticles as a function of their surface coating. *Biomaterials* 24, 1001–1011.
- Yang, S.-H., Sharrocks, A.D., Whitmarsh, A.J., 2003. Transcriptional regulation by the MAP kinase signaling cascades. *Gene* 320, 3–21.
- Zhao, C.M., Wang, W.X., 2011. Comparison of acute and chronic toxicity of silver nanoparticles and silver nitrate to *Daphnia magna*. *Environ. Toxicol. Chem.* 30, 885–892.
- Zhu, X., Zhou, J., Cai, Z., 2011. The toxicity and oxidative stress of TiO<sub>2</sub> nanoparticles in marine abalone (*Haliotis diversicolor supertexta*). *Mar. Pollut. Bull.* 63, 334–338.
- Zuur, A.F., Hilbe, J., Ieno, E.N., 2013. *A Beginner's Guide to GLM and GLMM with R: A Frequentist and Bayesian Perspective for Ecologists*. Highland Statistics.